THE CONFINEMENT EFFECT OF DIFFERENT GEOGRIDS

Nigel E Wrigley[1], Zheng Hong[2]

[1] *NewGrids Limited. Poole, BH14 9PW, UK (e-mail: nigel@newgrids.com)*
[2] *Technical Dept., BOSTD Geosynthetics Qingdao Ltd.: (e-mail: techcentre@bostd.com)*

Abstract: It is now well accepted that the primary fill stabilisation mechanism of geogrids is confinement of the fill by the geogrid. To gauge the potential for this and to compare products, index properties such as the load at 2% strain in each of the two primary directions have been used in the past. This approach has had some merit whilst all geogrids available were square or rectangular structures.

Now, however, the introduction of innovative products to the market has rendered this comparison ineffective. To overcome this, the option of doing tensile tests in more directions than just along the two primary axes has been proposed and used. However, this also is ineffective as it still fails to model the omni-directional confinement required to stabilise fill under a wheel load.

This paper shows that from index tests on the elements of a geogrid and a simple calculation, the confinement potential of different products can be readily determined and compared. The paper also shows that simply using tensile testing in different directions is inappropriate for this purpose.

Keywords: biaxial geogrids, index testing, reinforcement stiffness, reinforced road, soil reinforcement, stabilization,

INTRODUCTION

Biaxially stretched geogrids and woven/knitted grids have been used for the reinforcement of roads and other hardstandings over soft ground for more than 25 years. Their benefits and product differentiation have been widely studied and are now well understood (e.g. Jenner *et al*. 2002) but, as yet, it has not been possible to identify the exact product features that control this performance, differentiate various products and could be used in a rigorous design method. In seeking this many studies have been completed of which two key reports were Webster (1992) and Berg *et al* (2000). In Webster (1992) it was concluded that: *"The improvement mechanisms for geogrid reinforcement include grid interlock with aggregate base material, subgrade confinement, and to some extent a tensioned membrane effect"* By 2000, Berg *et al.* were able to refine this conclusion to: *"The primary mechanism associated with this application is lateral restraint or confinement"*. Since that time studies have progressed towards developing a design method for geogrid-reinforced roads. A key report in this field was Perkins *et al* (2004) in which aggregate confinement by the geogrid is recognised as being significant both during the initial compaction of the road base and also during subsequent performance in use.

In all these studies, high tensile modulus or stiffness of the geogrid is recognised as a key feature in generating effective confinement of aggregate. As a result, manufacturers promote the load at low-strain (typically 2%) of their geogrids as a key performance index. This has served the industry well until now as all geogrids had square apertures. With these a comparison of low-strain loads in the orthogonal machine and transverse directions of products gives an indication of their differing potentials for generating confinement of aggregate. However, a new biaxially-stretched geogrid with triangular apertures has now been introduced to some markets. With this product, testing in two orthogonal directions is clearly not directly related to its confinement potential. Therefore a different method of comparing the confinement forces that different geogrids can generate is now needed. This is the question addressed by this paper.

STRESSES INDUCED BY A WHEEL LOAD

Conventionally, the stresses induced in a road base by a wheel load are illustrated as shown in either Figure 1 or Figure 2.

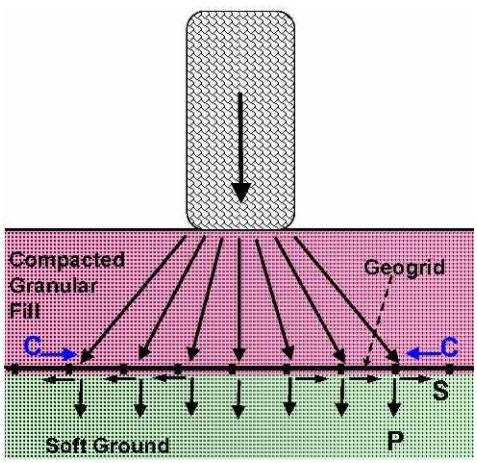

Figure 1: Wheel loading across a road

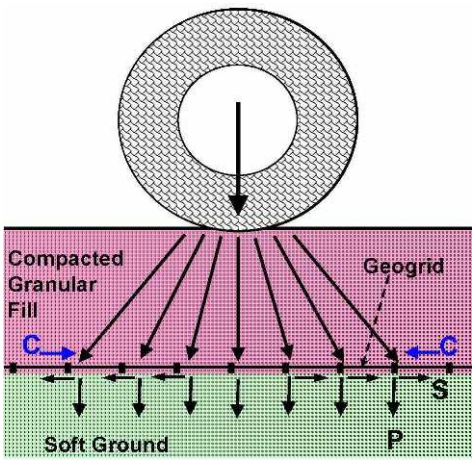

Figure 2: Wheel loading along a road

The stresses from the wheel load distribute down though the thickness of the road base to generate pressure P and shear stress S at the interface with soft ground. With an effective geogrid present at the interface a large proportion of the shear stress S is countered by a confining force C generated by the geogrid.

In such diagrams it appears that the situation can be analysed as a 2-dimensional stress field, but this is not the case. In plan view the wheel load can be modelled as a circular load, which at the ground interface is generating shear stresses S radiating uniformly and omni-directionally from the load centre as illustrated in Figure 3.

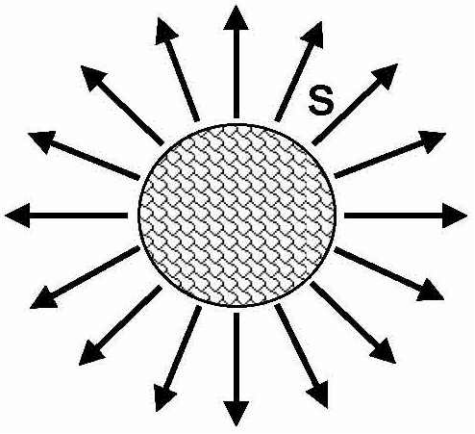

Figure 3: Plan view of shear stresses

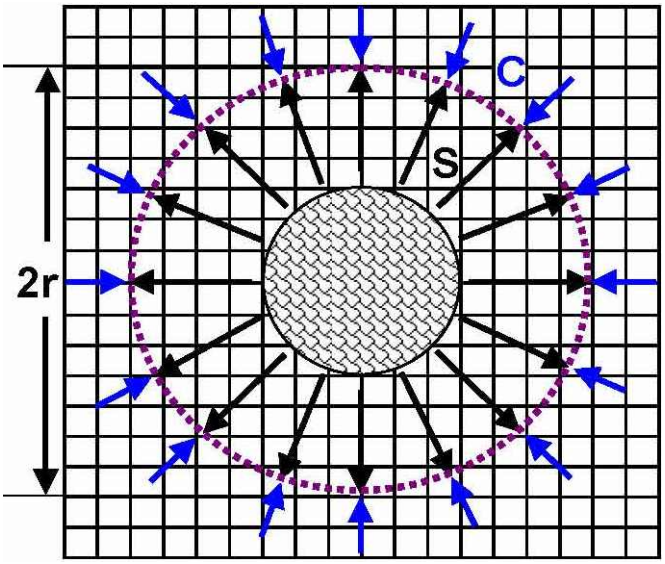

Figure 4: Plan view of shear stresses with geogrid present

The situation with an effective geogrid present is then illustrated in Figure 4. The shear stresses S stretch the geogrid uniformly in all directions over a circular area of radius r and the geogrid can be considered to be a circular element applying a confinement force C omni-directionally around this circle. Within this circle all ribs of the geogrid are stretched to the load appropriate to the strain applied. The question now is how to determine the magnitude and uniformity of the Confinement Force C that different geogrids can generate. Can it be done by direct testing? Or is a combination of test data and calculation needed? If it can be determined then this will yield a most useful index property that can be used to compare geogrids with differing aperture forms.

THE DETERMINATION OF CONFINEMENT FORCE C

Can C be determined by direct testing?

The index test method normally used by manufacturers to determine load at low strain for a geogrid is either ISO 10319 (ISO 1993) or ASTM D 6637-01 (ASTM 2001). These are conventional uni-directional tensile tests. ISO 10319 is purely a wide-width test with the test specimen having a width-length ration of around 2:1. ASTM D 6637-01 is more flexible as it also allows for single-rib testing. As written these tests may only be used orthogonally in the machine and longitudinal directions of a geogrid. But if they were to be used in other directions the results are illustrated in Figure 5.

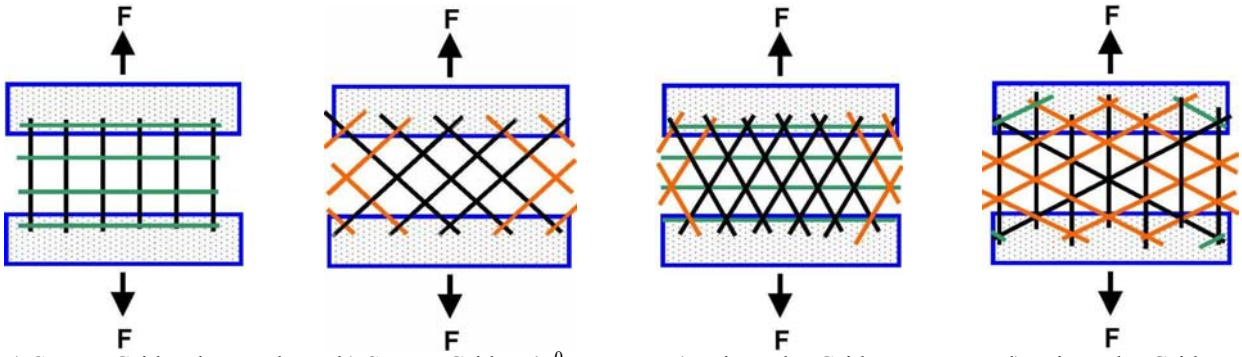

a) Square Grid orthogonal b) Square Grid at 45^0 c) Triangular Grid, MD d) Triangular Grid, TD

Figure 5: Schematics of wide-width testing

In figure 5 schematics are shown of various possible wide-width test orientations for both square and triangular aperture grids. There are three aspects of such uniaxial tests that are different from the omni-axial loading of the geogrid in Figure 4: number of ribs loaded, strain levels in ribs and junction rotation.

Number of ribs loaded:

If these drawings are compared to the situation of the loaded circle of geogrid in Figure 4 a significant difference between the two situations quickly becomes clear. In the loaded circle of geogrid all ribs are tensioned. Therefore at any section of the circumference of the circle all ribs at that section that are not parallel to the tangent to the circle contribute to the confining force C. In contrast, in the wide-width tests illustrated in Figure 5 only ribs that fully connect from one test jaw to the other contribute to the test load F measured. To highlight this the ribs on each test illustrated in Figure 5 have been colour-coded as follows:

- Black: ribs that contribute both to F in Figure 5 and to C in Figure 4
- Green: ribs that are parallel to the jaws and do not contribute to either F or C.
- Orange: ribs that contribute to C in Figure 4 but not to F in Figure 5

It can be clearly seen that the only test scenario in which the measured force F is a direct measure of the available confinement force C is Figure 5(a). This is representative of the four cardinal points of Figure 4 if the geogrid has square apertures. None of the tests with ribs at angles other than 90^0 to the edge of the jaws can be used to measure a force that is related to C.

Strain levels in ribs

The difference between F and C is also increased by strain differences in the two situations.

- In Figure 4 the whole circle of geogrid strains equally. Therefore, if the circle strains by 2%, each rib within it will strain also by 2% and contribute the appropriate load to C.
- In Figure 5, the strain in any rib that is not at 90^0 to the jaw is less than the jaw movement. This can be explained by reference to Figure 6.

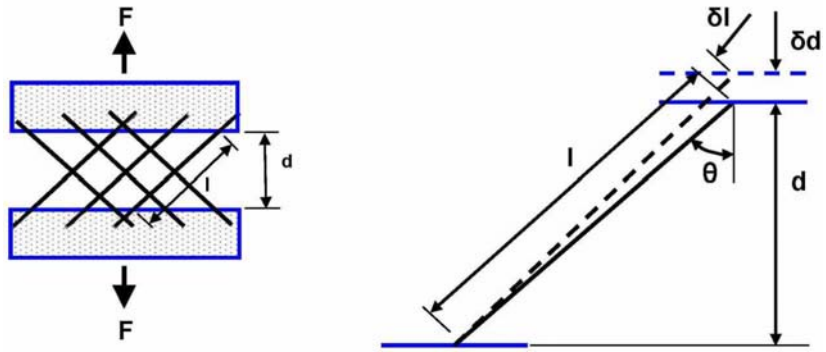

a) Tensioned ribs in Figure 5(b) b) Strain in an individual rib

Figure 6: Strains in angled ribs.

Figure 6(a) shows the test of Figure 5(b) with the non-tensioned ribs removed. The question of interest is: what is the strain in rib length l caused by an increase in jaw separation d. This is illustrated in Figure 6(b).

When the jaw separation increases by a small amount, δd, the extension of the rib, δl, is given by:

$\delta l = \delta d * \text{Cos}\theta$
and
$l = d/\text{Cos}\theta$

Therefore the strain in rib length l is given by

$\delta l/l = (\delta d/d) * (\text{Cos}\theta)^2$

Now, as Cos(45) is $1/\sqrt{2}$ then, for figure 6(a) or 5(b) if the jaws move apart by 2% the strain in the ribs is only 1%.

Junction Rotation:

The above two factors will both reduce the measured force F compared to the confining force C at the same nominal strain. There is then one factor that will increase F with some types of geogrid. This is junction rotation.

In figure 4 the uniform omni-axial load on the geogrid will give uniform expansion of the loaded circle of geogrid. Within this circle the angles between ribs will remain constant. If they start at 90^0, they will stay at 90^0 as the circle

expands. Equally, if the grid has equilateral triangular apertures the angles between ribs will start at $60^0$and remain at 60^0 as the circle expands.

By contrast, the uniaxial strain of the tests illustrated in Figures 5(b), 5(c) and 5(d) will cause the angles between ribs to change. Therefore, if the geogrid has stiff junctions that resist rotation then this will increase the measured force F needed to extend the geogrid.

Conclusion:

From the above discussion it can be clearly understood that there is no easily defined link between uniaxial index testing of a geogrid at different angles to its axes and the confinement force C it can generate in the omni-axial stress situation under a wheel load or any other form of point load.

The determination of C by calculation:

As discussed above, when the omni-axial stress S is applied to the geogrid the affected circle of geogrid will expand uniformly. This is the situation that applies if the geogrid has isotropic properties based on all ribs having similar properties and apertures being square or equilateral triangles. This is the case that will be covered in the rest of this paper. The principles of calculation described can be readily applied to geogrids with differing rib strengths and/or differing aperture dimensions in different directions, but, for the sake of clarity, that will not be discussed here.

Material properties needed for calculation

The confinement force C generated by a geogrid will obviously vary with the strain of the circle of loaded geogrid. Therefore it needs to be calculated either as a modulus or as a force at a given strain. Our preference is for the latter. Therefore we will concentrate in the rest of this paper on the determination of C_2 with the definition:

C_2 = The Confinement Potential of a Geogrid at 2% Strain

Now, if we are considering a strain of 2% for the circle of loaded geogrid, then all ribs within the circle will also be strained to 2%. Therefore the index property of the ribs needed for the calculation of C_2 is F_{R2} where:

F_{R2} = Rib Load at 2% strain

If F_{R2} and the pitch between ribs are known then C_2 can be calculated for all points around the circle of loaded geogrid as we will show below.

Measurement of F_{R2}:

Either wide-width or single-rib testing can be used to measure F_{R2}. Our preference would be wide-width, as by this, an average of a larger number of ribs will be determined. However, single-rib testing as defined in ASTM D 6637-01 (ASTM 2001) can be successfully used without modification to test representative ribs in all directions that they run.

For wide-width testing different considerations apply to triangular aperture geogrids from the established standard testing of square aperture geogrids. For the latter, tests carried out as illustrated in Figure 5(a) will generate the data needed to determine F_{R2}.

For Triangular aperture geogrids neither of the tests illustrated in Figures 5(c) and 5(d) will yield a measurement of individual rib strength as two or three sets of ribs are influencing F during test. Therefore tests with modified samples as illustrated in Figure 7 will be needed.

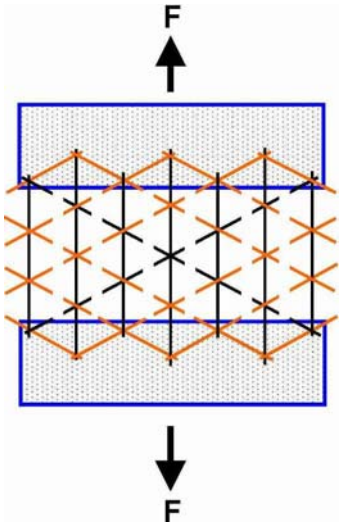

Figure 7: Modified wide-width test to determine individual rib strength in a triangular-aperture geogrid

In Figure 7 all ribs other than the set directly under test have been cut to eliminate any influence on F. From such tests on each set of ribs F_{R2} can be determined.

Calculation of C_2

Consider first one set of parallel ribs at a pitch of p and carrying a load of F_R each as illustrated in Figure 8.

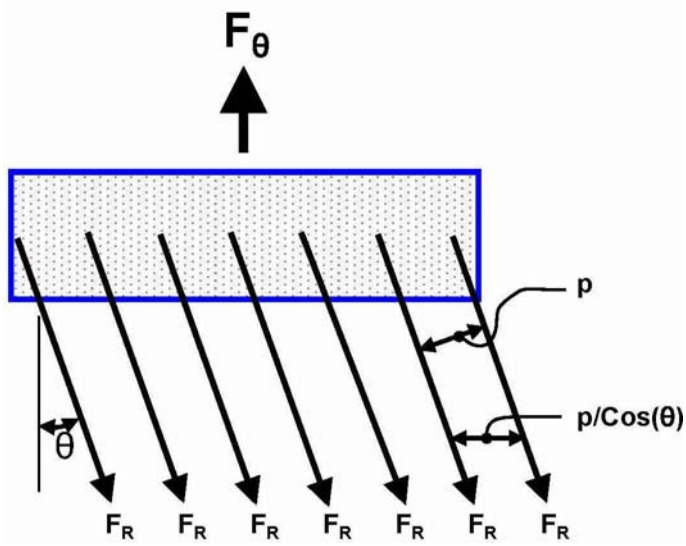

Figure 8: Forces from one set of ribs

In Figure 8 each rib contributes a force of (F_R*Cosθ) to Measured Load F_θ. Also, the spacing of the ribs across the jaw is given by (p/Cosθ). Therefore, F_θ is given by:

$$F_\theta = (F_R*\text{Cos}\theta)/ (p/\text{Cos}\theta) = (F_R/p)*(\text{Cos}\theta)^2 \text{ N/m} \quad (1)$$

Now consider the case of two sets of ribs at 90^0 to each other and both at pitch p as illustrated in Figure 9(a)

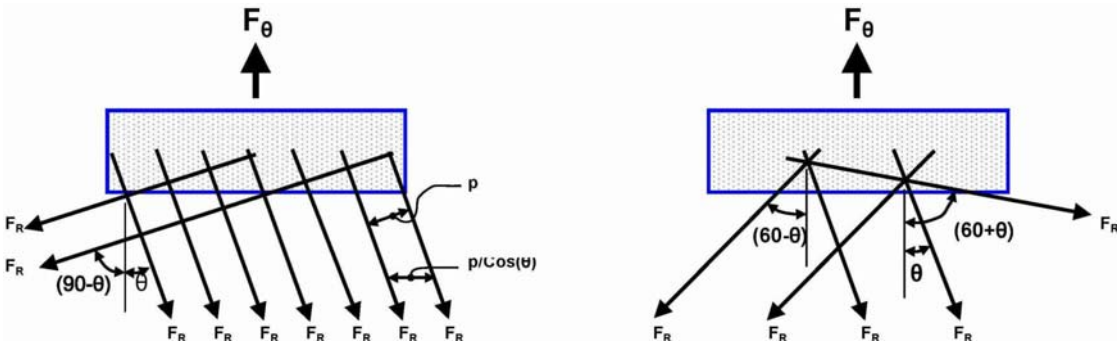

a) Two sets of ribs at 90^0 giving square apertures b) Three sets of ribs at 60^0 giving triangular apertures

Figure 9: Forces from multiple sets of ribs

In Figure 9(a) each set of ribs contributes to F_θ in accordance with Equation (1). Therefore the total value of F_θ is given by:

$$F_\theta = (F_R/p) * [(\text{Cos}\theta)^2 + (\text{Cos}(90-\theta))^2] \text{ N/m} \quad (2)$$

Now, by Pythagoras, $[(\text{Cos}\theta)^2 + (\text{Cos}(90-\theta))^2] = 1$, therefore if we substitute this together with C_2 and F_{R2} into Equation (2) we find that for all points around a loaded circle of a square aperture geogrid the Confinement Potential at 2% Strain of that geogrid is given by:

$$\mathbf{C_{2Square} = \frac{F_{R2}}{p}} \text{ N/m} \quad (3)$$

If we now consider the situation of 3 sets of ribs forming triangular apertures as illustrated in Figure 9(b) then by applying Equation (1) to each set F_θ in this case is given by:

$$F_\theta = (F_R/p) * [(Cos\theta)^2 + (Cos(60-\theta))^2 + (Cos(60+\theta))^2] \text{ N/m} \quad (4)$$

Now, if any value of θ is inserted into Equation (4) it is found that $[(Cos\theta)^2 + (Cos(60-\theta))^2 + (Cos(60+\theta))^2] = 1.5$ Therefore if we substitute this and C_2 and F_{R2} into Equation (4) we find that for all points around a loaded circle of a triangular aperture geogrid the Confinement Potential at 2% Strain of that geogrid is given by:

$$\mathbf{C_{2Tri} = 1.5 * \frac{F_{R2}}{p}} \text{ N/m} \quad (5)$$

CONCLUSIONS

- The Confinement Potential at 2% strain is a useful index property of a geogrid that can be compared across different types of geogrid. We would recommend that the IGS should ratify this new index property to give manufacturers, specifiers and users a common basis on which different products can be compared and judged.
- Equations (3) and (5) can be used to calculate the Confinement Potential at 2% of isotropic, square aperture and triangular aperture geogrids.
- The Confinement Potential at 2% of geogrids that are not isotropic can be calculated by applying Equation (1) to each set of ribs and summing the results
- Uniaxial tensile tests of a geogrid in directions other than along the principle axes of orthogonal grids do not give data that relates to the confinement potential of that geogrid in an omni-axial stress situation.

Acknowledgements: We thank BOSTD Geosynthetics Qingdao Ltd. for their support in the preparation of this paper.

Corresponding author: Mr Nigel E Wrigley, NewGrids Limited, 39 Clifton Road, Poole, BH14 9PW, United Kingdom. Tel: +44 1202 716493. Email: nigel@newgrids.com.

REFERENCES

ASTM 2001. Standard Test Method for Determining Tensile Properties of Geogrids by the Single or Multi-Rib Tensile Method. ASTM D 6637-01: ASTM, West Conshohocken, PA 19428-2959, United States.

Berg R R, Christopher B R, Perkins S, 2000. Geosynthetic reinforcement of the aggregate base/subbase courses of pavement structures. GMA White Paper II, Published for the Geosynthetic Materials Association by: Ryan R Berg & Associates, Woodbury, MN, USA

ISO 1993. Geotextiles: Wide-width Tensile Test. Internatonal Standard ISO 10319. ISO, Geneva, Switzerland

Jenner C G, Watts G R A, Blackman D I, 2002, Trafficking of reinforced, unpaved subbases over a controlled subgrade, Proceedings: Geosynthetics – 7th ICG, Swets & Zeitlinger, Lisse, Netherlands. pp 931-934

Perkins S W, Christopher B R, Cuelho E L, Eiksund G R, Hoff I, Schwartz C W, Svanø G, Watn A, 2004. Development of design methods for geosynthetic reinforced flexible pavements. FHWA Report Ref. DTFH61-01-X-00068. Department of Civil Engineering, Montana State University – Bozeman, Montana , USA

Webster S L, 1992. Geogrid reinforced base courses for flexible pavements for light aircraft: Test construction, behaviour under traffic, laboratory tests, and design criteria. DOT/FAA/RD-92/25, U.S. Department of Commerce, National Technical Information Service, Springfield, VA, USA